Experimental study on laser ignition of low vulnerability propellant based on nitrocellulose

Léo Courty[1], Jean-François Lagrange[1], Philippe Gillard[1], Christophe Boulnois[2]
[1] Univ. Orléans, PRISME EA 4229, Bourges, France
[2] Nexter Munitions, Bourges, France

1 Introduction

The use of energetic materials in propulsion field leads to several safety problems. Indeed, accidental stresses from thermal (fires) or mechanical (storage, transport) point of view can be of importance when it comes to ensure efficiency in spatial technologies. Today, very sensitive propellants are mainly used for propulsion. These powders can therefore lead to accidental situations and create important damages to the amenities and to human lives. Important accidents are those of the USS Oriskany (1966) and of the USS Enterprise (1696). To reduce the risk of accidental ignition, low sensitivity propellants have been developed in the early 90's. These powders allow better conditions of transport and storage than the "classical" ones. Nitrocellulose is used in the composition of several low sensitivity energetic materials. There are few data in the literature on the combustion and ignition of low vulnerability propellant. The aim of this work is to study laser ignition of such propellants. Combustion phenomena of propellant are complex and involve several processes, such as decomposition, oxidation, phase conversion, species diffusion, etc. In this context, several research works have been published over the past decades to clearly understand the combustion of propellants [1-11].

Price et al. [1] made a very complete review of all works performed in this field up to 1966. Ignition of solid materials is itself an important research topic, this is why Kulkarni et al. [2] and Hermance [3] listed all works related to solid ignition, both experimental and numerical works. A discussion on combustion general characteristics has been presented by Kubota [4] for different types of propellants. Similarly, Boggs [5] presented a review of knowledge on propellant combustion properties until 1984. More recently, Beckstead [6] reviewed numerical works dealing with solid propergol combustion. He summarized the different chemical kinetic models available and gave precisions on the different numerical schemes used and their comparison. Miller [7] developed a simple ideal 1D model for the simulation of the combustion of homogeneous solid materials. His formulation is made of several analytical approximations that lead to the empirical formulation of the pressure dependency related to combustion rate.

Atwood et al. [8] presented data on combustion rate from measurements performed with the most famous solid propergols. They also made a database analysis to obtain the sensitivity of combustion rate on temperature [9]. In a recent work, Miller [10] studied in details several questions related to propellant

combustion rate calculations from numerical models, highlighting the effect of chemistry in condensed phase. Cor and Branch [11] worked on flame kinetic chemistry on propellant surface in numerical models used until 1995.
Ignition energies are studied in this work using a laser diode. Results are given for different laser powers. The effects of initial pressure on the overpressure and ignition time are also given. Used propellant and experimental setup are described in the next section. Results and discussions are presented in section three.

2 Materials and methods

Nitrocellulose based propellant

Experiments were performed with cylindrical pellets made of nitrocellulose (~98 %) and diphenylamine (~1.2 %). These pellets are commercial propellants given by Airbus Safran Launchers and used as received. Their average diameter, length and mass were respectively 5.4 mm, 11.4 mm and 355 mg. Each cylinder is perforated and composed of 7 holes. A scheme of the used propellant is presented in Figure 1.

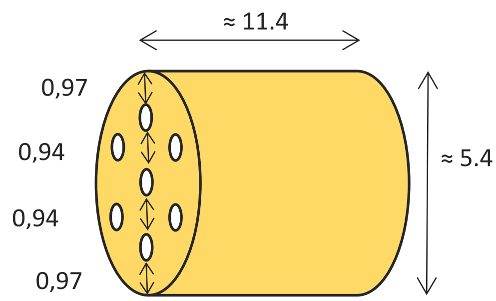

Figure 1. Picture and scheme of the used propellant.

Experimental setup

Experimental setup consists in a stainless steel cylindrical reactor coupled to a laser diode, optical system, a photodiode, an optical spectrometer and a pressure sensor. An overview of the setup is presented in Figure 2. Internal volume of the reactor is of 55 cm^3 and it is possible to open it from the control room for users' safety. A Coherent laser diode (FAP-I-P1396) operating at 808 nm is used for ignition. An optical fiber brings the laser beam to the optical system that consists in two lenses, in order to obtain a laser spot size on the sample of a diameter of 1.25 mm. Optical system consists in two lenses with focal lengths of respectively 16 and 25 mm. Pressure sensor (Kistler, 603B) and photodiode are connected to a digital oscilloscope (Agilent Technologies, DSO-X 3034A).
An experiment is conducted as follows: a propellant sample is placed in a PMMA holder (length 28 mm), this holder is placed in the reactor and closed with a sapphire window. Samples are placed in order not to have any space between sample and window. Reactor closed with the sapphire window was tested to resist to a pressure of 250 bars during 15 min. Selected initial pressure of the selected atmosphere is set, laser energy is brought and pressure and photodiode signals are recorded if ignition occurs. Two atmospheres are used for the initial pressure: nitrogen and argon. Initial pressure is varied between 10 and 70 bars for both gases. Laser pulse duration can be varied with the Coherent laser diode. Laser power can be varied by changing laser current, laser temperature is fixed at 20 °C. Five powers were studied: 0.66, 1.43, 2.86 and 9.95 W that correspond respectively to laser current intensity of 9, 10, 12 and 22 A.

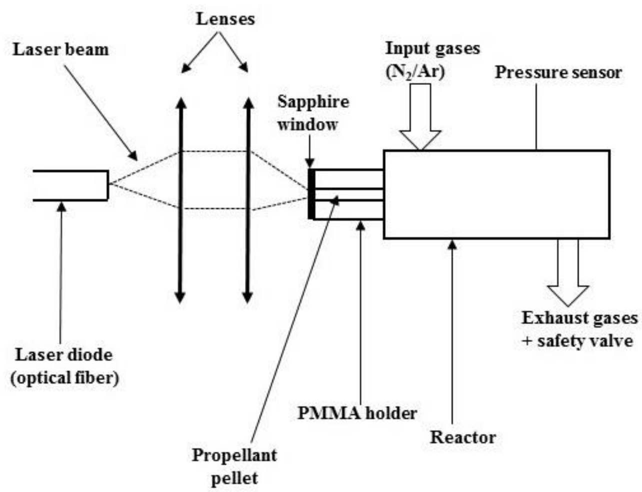

Figure 2. Scheme of the experimental setup

3 Results and discussions

Results on overpressure, propagation rate, ignition time and minimum ignition energy are presented for different laser powers and the two studied atmospheres: nitrogen and argon.

Effect of initial pressure

Figure 3 presents overpressures as functions of initial pressure for the two studied atmosphere (a) and an example of obtained pressure signals at an initial pressure of 70 bars (b). Definition of t_i and ΔP are given in Figure 3b. Obtained overpressures are divided by the mass of the pellet. It is clear reading this figure that overpressures are increasing when initial pressure is increasing up to approximately 45 bars. Between 45 and 50 bars, overpressure is constant or slightly decreasing when initial pressure is increasing. For initial pressures higher than 50 bars, an increase of initial pressure leads to an increase of obtained overpressure. It is also clear reading this figure that obtained overpressures are higher under argon atmosphere than under nitrogen atmosphere. Argon can be seen as a combustion enhancer for this kind of propellant, as already noticed in the literature [12]. This effect can be due to the reactions of nitrogen that might consume a part of the generated thermal energy, therefore leading to lower combustion temperature and pressure. On the contrary, argon might behave as almost inert.

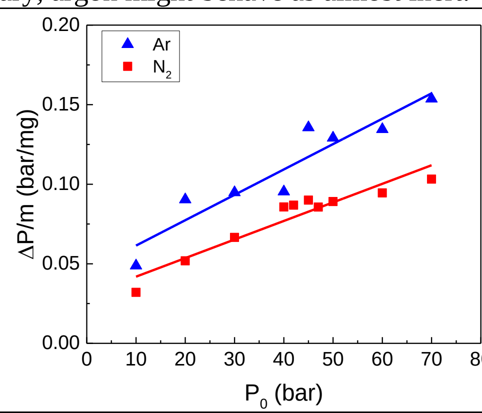	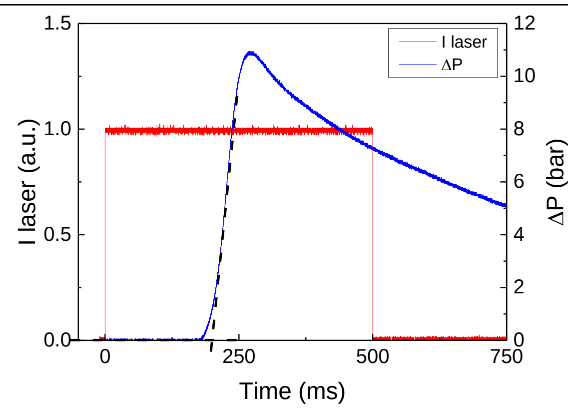
(a)	*(b)*

Figure 3. Overpressure as a function of initial pressure under nitrogen and argon atmospheres (a) and an example of obtained pressure signal.

Propagation rate is estimated by measuring $\frac{1}{m}.\left(\frac{d\Delta P}{dt}\right)_{max}$ and ignition delay t_i is obtained thanks to pressure signal. It is defined as the time between the beginning of the laser shot and the beginning of pressure increase. Figure 4 presents propagation rate (a) and ignition delay (b) as functions of the initial pressure.

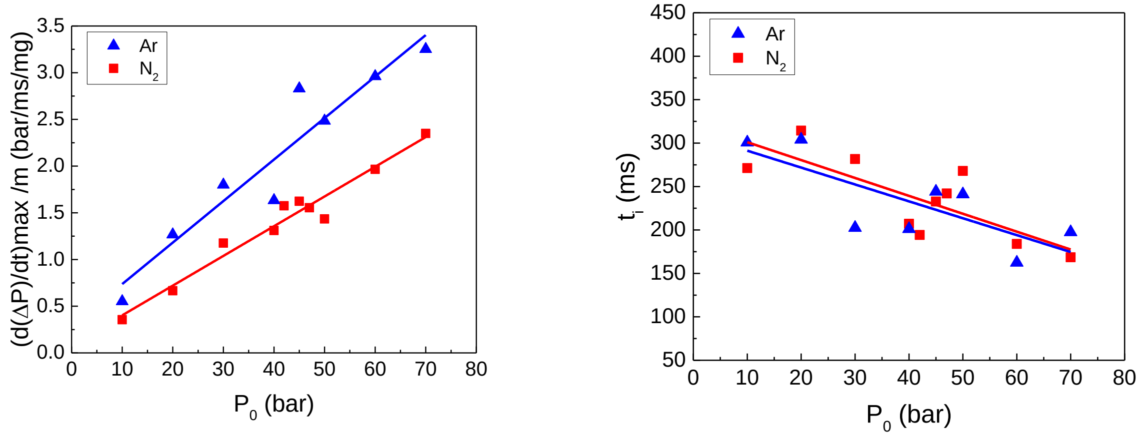

(a) *(b)*

Figure 4. Propagation rate *(a)* and ignition delay *(b)* as functions of initial pressure under nitrogen and argon atmospheres.

We can see in Figure 4 that propagation rate is behaving similarly to overpressure as a function of initial pressure: it is increasing linearly up to 40 bars, then decreasing between 40 and 50 bars, and then increasing again linearly above 50 bars. Propagation rate is higher in argon than in nitrogen for all studied initial pressures. Concerning ignition delays, we can say that there is no clear differences between shots under argon and nitrogen atmospheres. Above an initial pressure of 20 bars, ignition delays tend to decrease when initial pressure is increasing: ignition delays at 70 bars are 66% lower than those at 10 bars. This is just a tendency because we can observe some increases for some initial pressures.

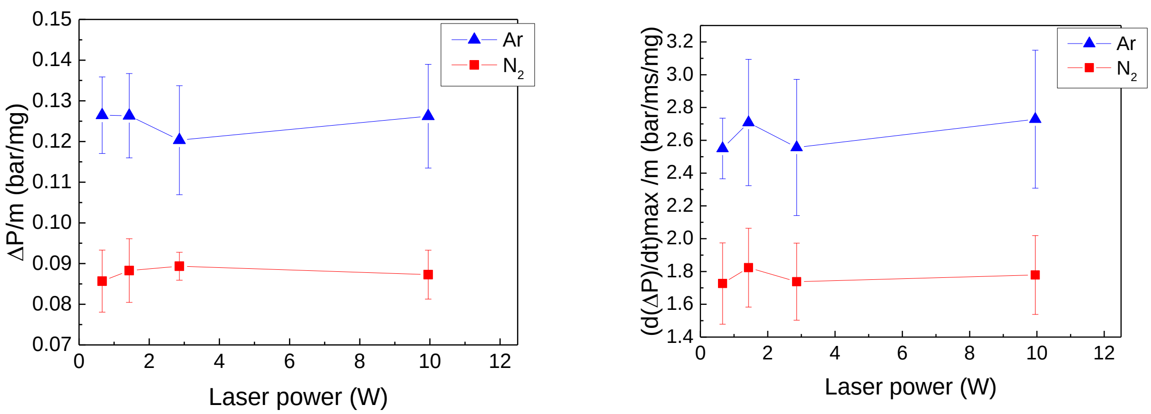

(a) *(b)*

Figure 5. Overpressure and propagation rate as functions of laser power under nitrogen and argon atmospheres.

Effect of laser power

Figure 5 presents overpressure (a) and propagation rate (b) of studied propellant as functions of laser power under the two studied atmospheres (nitrogen and argon) at an initial pressure of 50 bars. We can say that there is almost no effect of laser power on these two parameters: the relative deviation does not exceed 4%. We can also notice that values under argon are more important than under nitrogen: overpressure are higher and combustion speed is also higher under argon.

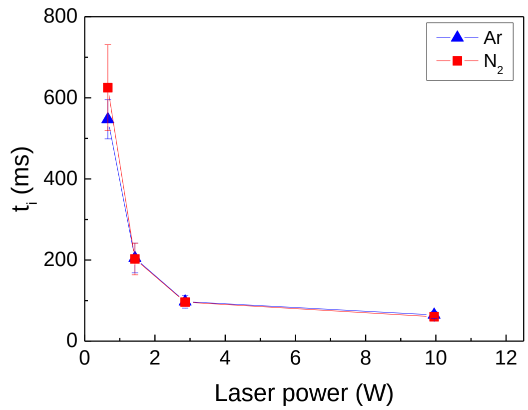

Figure 6. Ignition delay as a function of laser power under nitrogen and argon atmospheres.

Ignition delays as functions of laser power are presented in Figure 6 for the two studied atmospheres. Similarly to initial pressure effect, we can say that ignition delays are the same under argon and nitrogen atmospheres, there is no effect of the gaseous atmosphere. As expected, ignition delays are decreasing when laser power is increasing. The slope is very high for three lowest power values, and t_i is very slightly decreasing between 6.42 and 9.95 W. Interestingly, standard deviations are strongly decreasing with laser powers as it can be seen in the error bars.

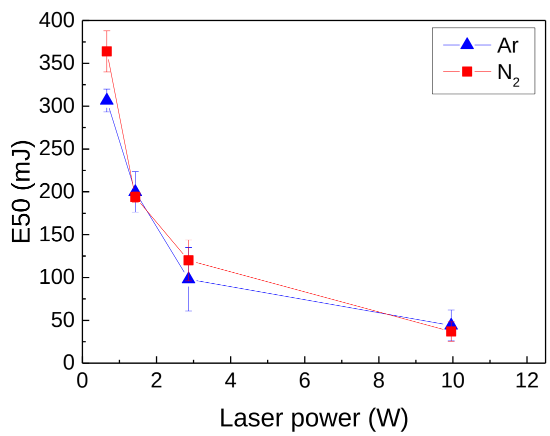

Figure 7. E_{50} as a function of laser power under nitrogen and argon atmospheres.

Ignition energies

Ignition probabilities as functions of deposited energies are studied in this paper as functions of different power lasers. For a given power, energies giving 50 % of probability of ignition (E_{50}) are investigated (and E_{05} and E_{95}, respectively energies giving 5 and 95 % of ignition probability are deduced from E_{50}). Langlie

method [13] has been adopted in this work. This method is based on dichotomy principle and relies on a statistical repartition of ignition threshold following a standard normal distribution. Thanks to this method, we can obtain E_{50} parameter with 20 to 30 shoots.
E_{50} as functions of laser power are plotted in Figure 7 for the two studied atmospheres at an initial pressure of 50 bars. Propellant needs globally more energy to be ignited in nitrogen than in argon but the effect of gaseous atmosphere is not very important. E_{50} is decreasing when laser power is increasing for both gases. Under nitrogen and argon, E_{50} are respectively of 363.91 and 306.58 mJ at 0.66 W and respectively of 36.88 and 42.02 mJ at 9.95W. Associated standard deviations are respectively of 23.94 and 13.37 mJ at 0.66 W and respectively of 11.34 and 18.06 mJ at 9.95 W.

Acknowledgment: *Authors want to thank the 'Conseil Régional du Centre Val de Loire', in France, which has financially supported this work (LILOVEM Project).*

References

[1] Price EW, Bradley HHJ, Dehority GL, Ibiricu MM. (1966). Theory of Ignition of Solid Propellants. AIAA Journal. 4(7): 1153-1181.

[2] Kulkarni AK, Kumar M, Kuo KK. (1982). Review of Solid-Propellant Ignition Studies. AIAA Journal. 20(2): 243-244.

[3] Hermance CE. (1984). Solid-Propellant Ignition Theories and Experiments, in Fundamentals of Solid Propellant Combustion, Kuo KK and Summerfield M, eds., AIAA Progress in Astronautics and Aeronautics Series. 90: 239-304.

[4] Kubota N. (1984). Survey of Rocket Propellants and Their Combustion Characteristics, in Fundamentals of Solid Propellant Combustion, Kuo KK and Summerfield M, eds., AIAA Progress in Astronautics and Aeronautics Series. 90: 1-52.

[5] Boggs TL. (1984). The Thermal Behavior of Cyclotrimethylene-trinitramine (RDX) and Cyclotetramethylene-tetranitramine (HMX), Fundamentals of Solid Propellant Combustion, Kuo KK and Summerfield M, eds., AIAA Progress in Astronautics and Aeronautics Series. 90: 121-175.

[6] Beckstead M. (2006). Recent Progress in Modeling Solid Propellant Combustion. Combustion, Explosion, and Shock Waves. 90(6): 623-641.

[7] Miller MS. (1982). In Search of an Idealized Model of Homogeneous Solid Propellant Combustion. Combustion and Flame. 46: 51-72.

[8] Atwood AI, Boggs TL, Curran PO, Parr TP, Hason-Parr DM. (1999). Burning Rate of Solid Propellant Ingredients, Part 1: Pressure and Initial Temperature Effects. Journal of Propulsion and Power. 15(6): 740-747.

[9] Atwood AI, Boggs TL, Curran PO, Parr TP, Hason-Parr DM. (1999). Burning Rate of Solid Propellant Ingredients, Part 2: Determination of Burning Rate Temperature Sensitivity. Journal of Propulsion and Power. 15(6): 748-752.

[10] Miller MS. (2003). Burning Rate Models and their Successors: A Personal Perspective, Technical Report, ARL-TR-2996, Army Research Laboratory.

[11] Cor JJ, Brach MR. (1995). Structure and Chemical Kinetics of Flames supported by Solid Propellant Combustion, Journal of Propulsion and Power. 11(4): 704-716.

[12] Mar M, Gillard P, Courty L. (2015). Numerical simulations of ignition and combustion of RDX mixed with gaseous additives. 25th ICDERS. Leeds, UK.

[13] Langlie H.J. (1962). A reliability Test Method for One Shot items. Ford Motor Company Aeronutronic – Publication n° U1792.